J Neurophysiol 133: 1886–1901, 2025.
First published May 5, 2025; doi:10.1152/jn.00461.2024

american physiological society

JNP JOURNAL OF NEUROPHYSIOLOGY

RESEARCH ARTICLE

Integrative Research on the Functional Logic of Neural Circuits

Acute effects of orofacial, neck, and shoulder relaxation exercises and chewing on soleus H-reflex and motor unit discharge patterns

Marša Magdič,[1] Aleš Holobar,[2] Matej Kramberger,[2] Matjaž Vogrin,[1,3] Nina Murks,[2] Anita Fekonja,[1,4] and Miloš Kalc[5]

[1]*Faculty of Medicine, University of Maribor, Maribor, Slovenia;* [2]*Faculty of Electrical Engineering and Computer Science, University of Maribor, Maribor, Slovenia;* [3]*Department of Orthopaedics, University Medical Centre Maribor, Maribor, Slovenia;* [4]*Department of Orthodontic, Community Health Centre Maribor, Maribor, Slovenia; and* [5]*Institute for Kinesiology Research, Science and Research Centre of Koper, Koper, Slovenia*

Abstract

The interconnected nature of orofacial, neck musculature, and the neural system suggests that localized activities, such as teeth clenching, can influence remote spinal excitability. Although stretching exercises are known to have both local and remote effects, the specific impact of orofacial muscle stretching remains underexplored. This study investigates the effects of two interventions: 25 guided orofacial and neck stretching and mobility exercises (exercises), and chewing six chewing gums for six minutes (chewing), on the soleus H-reflex and D1 presynaptic inhibition. Ten volunteers (mean age: 28.75 ± 9 yr) participated, with H-reflex measurements collected using high-density electromyography (HDsEMG) before and after each intervention. Latency (H_{LAT}), duration (H_{DUR}), peak-to-peak (H_{P2P}, $D1_{P2P}$), and positive peak (H_{POS}) amplitudes were extracted from unconditioned and conditioned H-reflexes. The ratio ($D1_{P2P}/H_{P2P}$) between conditioned ($D1_{P2P}$) and unconditioned (H_{P2P}) H-reflex was calculated to study the D1 presynaptic inhibition mechanisms. In addition, 8,400 firings from 376 distinct motor units (MUs), categorized by firing threshold were analyzed for latency, firing ratio, and inhibition probability ($D1_{PROB}$). H_{P2P}, H_{POS} decreased and H_{DUR} was significantly increased after the exercise intervention, whereas the chewing intervention had no effect on these parameters. The $D1_{P2P}/H_{P2P}$ ratio and $D1_{PROB}$ remained unchanged, suggesting that the observed drop in H_{P2P} is not mediated by presynaptic inhibition mechanisms. Single MU analysis confirmed the H-reflex findings. The results of this study suggest that stretching and mobility exercises targeting the neck and orofacial region can reduce neuromuscular excitability, offering potential for nonpharmacological management of conditions associated with motoneuron hyperexcitability and general whole body relaxation.

NEW & NOTEWORTHY This study provides the first evidence that orofacial and neck mobility exercises can acutely reduce spinal excitability in remote lower-limb muscles. By combining high-density surface EMG with both global and single motor unit H-reflex analyses, we demonstrate a decrease in soleus H-reflex amplitude independent of presynaptic inhibition. These findings suggest potential nonpharmacological applications for managing motoneuron hyperexcitability and promoting whole body relaxation in individuals with cervical and orofacial constraints.

high-density electromyography (HDsEMG); mobility exercises; remote effect; stretching; teeth clenching

INTRODUCTION

Remote influences on spinal reflex excitability have long been recognized in neurophysiology. A classic example is the Jendrassik maneuver, where voluntary contraction of distant muscle groups (e.g., teeth clenching) significantly enhances the stretch reflex in the lower limbs (1, 2). Modern imaging techniques, like functional magnetic resonance imaging (fMRI), have enabled deeper investigation of neural mechanisms, demonstrating that teeth clenching activates a broad cortical network and facilitates communication between distinct motor areas of the brain (3, 4). This activity

Correspondence: M. Magdič (marsa.magdic@gmail.com); M. Kalc (milos.kalc@zrs-kp.si).
Submitted 10 October 2024 / Revised 19 December 2024 / Accepted 26 April 2025

affects voluntary motor output by modulating the excitability of neurons in the motor cortex and spinal motoneuron pool (5), potentially engaging cortical and subcortical pathways (2, 6). Early hypotheses attributed the effects of the Jendrassik maneuver to an increased fusimotor (γ-motor) drive, heightening muscle spindle sensitivity (7). However, the fact that the Jendrassik maneuver facilitation is observed even for the H-reflex (a monosynaptic reflex bypassing the muscle spindle) suggests that central gating mechanisms are at play (8). In particular, a reduction in presynaptic inhibition of Ia afferents has been proposed as a key mechanism for the reflex enhancement during Jendrassik maneuver (8).

Beyond the Jendrassik maneuver, other forms of remote muscle activation or stretching produce similar modulatory effects on the spinal cord. For instance, prolonged unilateral muscle stretching can induce not only an increase in the range of motion (ROM) of the stretched muscle, but also induces moderate ROM increase to contralateral, nonstretched limbs (9–13), likely through physiological mechanisms such as heightened stretch tolerance or reduced sympathetic excitation (9). Moreover, some studies have reported that stretching a muscle on one side may decrease maximal force output or reflex excitability also on the contralateral side (9–13). Notably, because the contralateral limb is not mechanically stretched, any observed "crossover" effects must arise from neural mechanisms rather than peripheral muscle factors (10, 14). The current literature suggests that both spinal and supraspinal mechanisms may contribute to remote reflex depression after remote stretching. Among the possible underlying mechanisms, the proposed explanation involves central neural system adjustment leading to a reduction in α-motoneuron pool excitability in the contralateral limb (10), possibly driven by an increase in presynaptic or other inhibitory mechanisms acting on contralateral Ia terminals, thereby depressing the stretch reflex sensitivity across the spinal cord. On the other hand, supraspinal influences are also likely involved (10). In addition to teeth clenching and passive stretching, rhythmic oral motor activity such as mastication has also been shown to modulate spinal reflex excitability (15). Although less extensively studied, research suggests that chewing may facilitate the soleus H-reflex during the activity itself. For example, Takahashi et al. (15) reported an increase in H-reflex amplitude during mastication, which they attributed to tonic, nonreciprocal facilitation of the motoneuron pool potentially driven by jaw muscle spindle afferents. Similarly, Hagiya (16) proposed that rhythmic chewing may enhance H-reflex excitability via descending input from the pontobulbar reticular formation.

Given the strong effects provided by the activation of orofacial muscles (e.g., the Jendrassik maneuver or chewing) and the remote effect of stretching, one would expect that stretching or rhythmic activation of orofacial muscles could significantly influence the remote neuromuscular system, inhibiting or facilitating remote reflex responses, respectively. Indeed, recent evidence suggests that the relaxation of neck and orofacial muscles can improve active ROM and balance (17). However, despite evidence of muscle stretching- and teeth clenching-induced remote neural effects, the combination of both effects, i.e., the effects of orofacial muscle stretching and on the remote neuromuscular system, is poorly investigated.

Among noninvasive methods to assess spinal mechanisms, the Hoffmann or H-reflex is a valuable tool (18). This method assesses the effectiveness of Ia afferents in eliciting motoneuron excitatory postsynaptic potentials (EPSPs), which are modulated by various synaptic pathways (19). Presynaptic and postsynaptic mechanisms can influence the motoneuron pool excitability, defining the reflex amplitude (19). For example, it is thought that stretching reduces the H-reflex amplitude in both stretched and remote muscles (9, 10, 12–14), whereas teeth clenching increases the soleus muscle (SOL) H-reflex amplitude (2, 3).

Although the H-reflex is a widely used assessment tool, the interpretation of the results could be confounded by different spinal mechanisms at the presynaptic and postsynaptic levels. A key modulatory process is the presynaptic inhibition of Ia afferent terminals, which adjusts the efficacy of sensory input transmission to motoneurons (20). Both central and peripheral inputs critically regulate presynaptic inhibition. For instance, descending pathways from supraspinal centers modulate the excitability of primary afferent depolarization (PAD) interneurons, attenuating or enhancing Ia-terminal inhibition depending on task demands (20).

A fundamental challenge in H-reflex studies is differentiating presynaptic modulation from postsynaptic changes when reflex amplitude is altered. A decrease in the compound H-reflex could result from enhanced presynaptic inhibition of Ia afferents, but it could equally arise from decreased motoneuron pool excitability or other synaptic influences (19). Traditional electrophysiological techniques have used conditioning stimuli to address this issue. For instance, delivering a modest conditioning volley to an antagonistic nerve can evoke the so-called D1 and D2 inhibition of the H-reflex (with early and late phases of 5–30 ms and 70–200 ms, respectively) (21), phenomena attributed largely to presynaptic inhibition of Ia terminals (22). By comparing the peak-to-peak amplitude of an H-reflex with and without conditioning, presynaptic inhibition can be inferred: stronger conditioned reflex depression indicates greater presynaptic inhibitory drive and vice versa. However, compound H-reflex measurements and conditioning paradigms have important limitations. Postsynaptic effects can temporally overlap with presynaptic inhibition (20), confounding the interpretation of conditioned reflex changes. For example, a long-latency facilitatory effect from cutaneous afferents (induced by the electrical stimuli) can occur alongside the presynaptic inhibitory phase, making the net inhibition seem smaller and potentially masking true presynaptic changes (23). In addition, changes in motor units (MUs) recruitment gain, represented by shifts in recruitment thresholds, can mimic reflex size changes without actually inducing presynaptic modulation (20).

To resolve these ambiguities, Hultborn et al.'s (23) seminal work demonstrated that, within the first 0.6 ms of the H-reflex response, monosynaptic Ia excitation remains uncontaminated by disynaptic inputs, and reflex facilitation depends solely on the size of the conditioning Ia EPSP. The most reliable method to exclude MU recruitment gain changes is to confirm compound H-reflex findings with peristimulus time histograms (PSTHs) of single MU firings. To address these challenges, we incorporated the analysis of single MU responses extracted from high-density surface electromyography (HDsEMG) recordings in elicited

contractions, a computational technique recently developed by our group (24, 25).

Given the intricate relationship between orofacial and cervical muscles and their influence on neuromuscular control, this study aimed to explore the effects of a guided mobilization (static and dynamic stretching) exercise protocol targeting orofacial and neck muscles, and the impact of chewing on the soleus H-reflex. We also investigate associated changes in MU discharge patterns. Based on prior evidence, we hypothesize that the mobilization protocol will reduce soleus H-reflex amplitude, whereas chewing will increase H-reflex amplitude, reflecting distinct neural mechanisms.

MATERIALS AND METHODS

Ten healthy volunteers (age: 28.75 ± 9 yr) participated in this study. The exclusion criteria were known muscular and neurological disorders, pregnancy, temporomandibular disorder [scored > 15 on the Fonseca Anamnestic Index (FAI)], and/or previous orthodontic treatments. The FAI is a validated questionnaire used to screen for temporomandibular disorders, with scores above 15 indicating significant symptoms. Participants were instructed to abstain from coffee and alcohol on the assessment day. The research was approved by the Medical Ethics Committee of the Republic of Slovenia (No. 0120-417/2021/3). The study was conducted in accordance with the Declaration of Helsinki. All the participants gave their written consent before the examination.

Study Design

The present study operated as a crossover, repeated-measures design. In a single visit, each subject participated in two different intervention protocols. After a short warm-up, a preintervention procedure was held (later explained in detail). For the interventions, the participants were asked to sit on an ankle dynamometer and perform: *1*) a guided series of exercises directed at ameliorating intramuscular coordination of muscles directly or indirectly involved in mastication and maintaining head posture (exercise), and *2*) active chewing of chewing gums for 6 min (chewing). Between exercise and chewing interventions, a 20-min wash-out period was included to reduce lingering effects (Fig. 1*A*). The extent of the rest period was tested in a previous pilot study. All the subjects were equipped with electrodes for *1*) bi-polar electromyography (biEMG) and *2*) high-density surface electromyography (HDsEMG). Before and after each intervention, unconditioned and conditioned H-reflexes were assessed without background muscle activity.

EMG Measurements

The skin over the soleus muscle belly was shaved, abraded with an abrasive paste and cleansed with water. A semi-disposable adhesive matrix electrode (5 × 13 electrodes; GR08MM1305, OT Bioelettronica, Italy, interelectrode distance of 8 mm) was placed in the position that has been proposed as the most suitable to obtain the largest amplitude of the H-reflex, with the long side of the array parallel with the longitudinal axis of the muscle (26). A wet-soaked strap reference electrode (WS2, OT Bioelettronica, Italy) was fixated around the ankle and the supplementary ground electrode (5 × 3 cm, T3545, OT Bioelettronica, Italy) on the tuberositas tibiae just under the patellar ligament.

To monitor the muscular activity and quality of the electrophysiological signals, we used another bipolar EMG (biEMG) system. Single-use recording electrodes (Covidien 24 mm, Walpole, MA) were applied in the proposed standard bipolar configuration lateral to the HDsEMG array (27). The reference electrode (50 × 100 mm, 00734, Complex, Guildfor, UK) was placed over the patella.

The Quattrocento acquisition system (sampling rate of 5,120 Hz, 16-bit resolution) coupled with the OTBioLab + software (both OT Bioelettronica, Torino, Italy) were used to collect the HDsEMG signals. The PowerLab toolbox (sampling rate of 4,000 Hz) and LabChart 8 software (both ADInstruments, Australia) were used to collect biEMG signals. Signals were band-pass filtered (10–500 Hz).

For the entire duration of the experiment, the subjects sat in an ankle dynamometer equipped with a force sensor (Wise Technologies, Ljubljana, Slovenia). The hips, knees, and ankles were each positioned at a 90° angle. Their feet were secured using a fixation system on the thigh and straps over the instep (Fig. 1*B*). Participants were instructed to remain relaxed, avoid clenching their teeth or squeezing their hands, and keep their head and forearms in the same position, with forearms supported.

Warm-Up and Preliminary Force Tracking Procedure

The warm-up consisted of several contractions of the plantar flexors. In detail, seven contractions for 5 s each, with a 30-s pause between contractions, ranging from 50% to nearly maximal intensity, subjectively estimated, were executed. After 60 s of rest, maximal voluntary contraction (MVC) was determined. Participants were instructed to gradually contract the plantar flexors over 1–2 s, maintaining maximal force for 3 s (repeated twice with 120 s of rest in between). A 120-s rest period followed. Subsequently, participants performed a visuomotor force tracking task, maintaining force for 20 s at 10%, 20%, and 30% of MVC, and for 15 s at 40%, 50%, and 70% of MVC, with 120 s of rest between contractions to prevent fatigue. This task was crucial for defining MU filters, which facilitate the recognition of MUs during elicited contractions (24). Participants followed a display in front of them, which showed two beams: one indicating the target force and another, in a different color, which they controlled by exerting plantar flexion torque.

Peripheral Nerve Stimulation

A custom-built current-driven high-voltage electrical stimulator (Stim_1, EMF-Furlan, Slovenia) was used to deliver individual rectangular electrical impulses (1 ms) to the tibial nerve in the popliteal fossa, which evoked H-reflexes in the right soleus (SOL). First, we determined the ideal stimulation point of the tibial nerve using a stimulation pen. On the assessed point, we applied a self-adhesive electrode (25 mm diameter, J10R00, Axelgaard Manufacturing Co., Lystrup, Denmark), which acted as a cathode. The anode (50 × 90 mm, MyoTrode PLUS, Globus, Italy) was set over the patella.

After the force tracking procedure, we acquired the H-reflex and M-wave (HM) recruitment curve. We started the

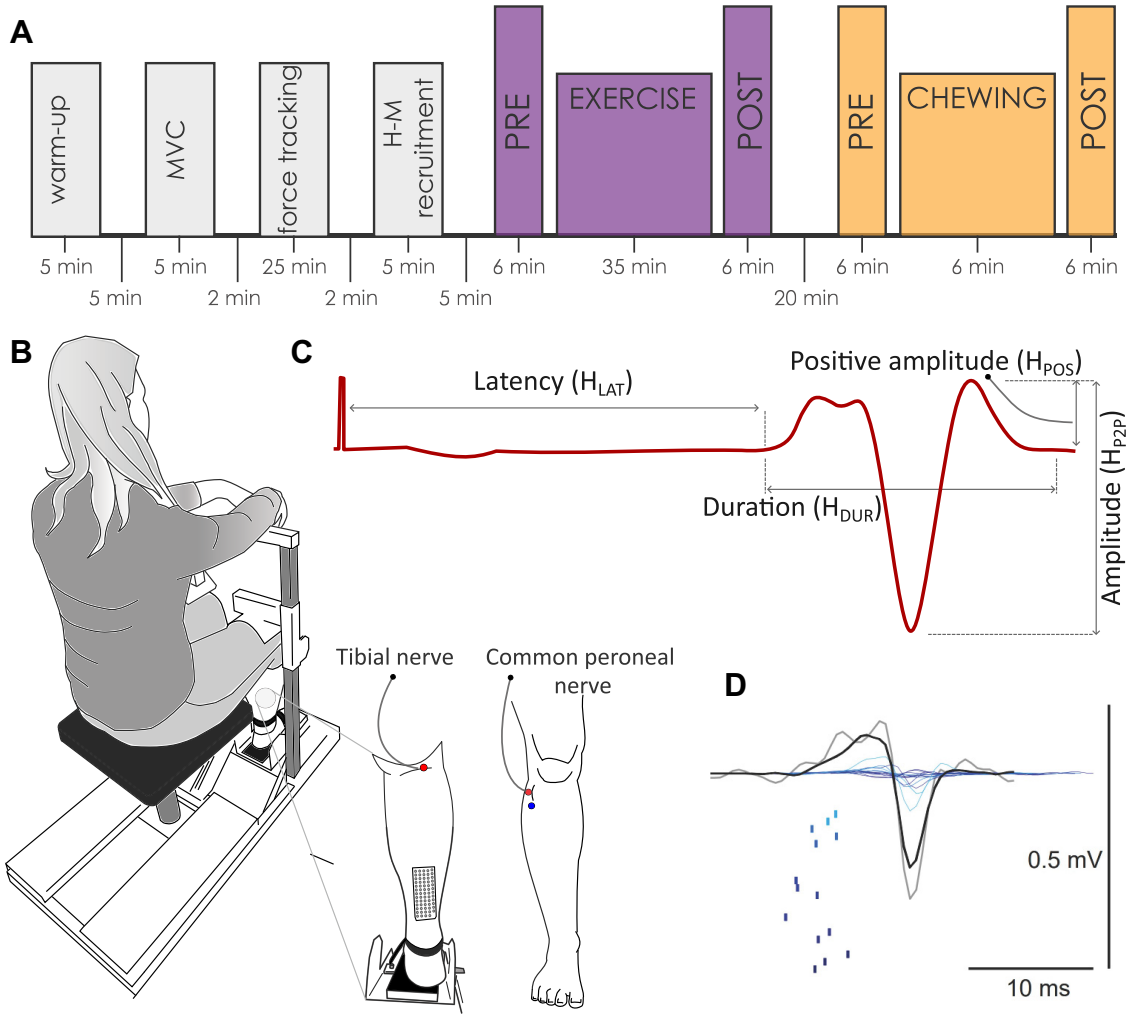

Figure 1. Study design and methodology used in this study. *A*: schematic representation of the study design. *B*: participant positioning during the experiment, including details of the array electrode placement and stimulation electrodes on the tibial nerve (in the popliteal fossa) and the common peroneal nerve. *C*: representative H-reflex response with extracted parameters. *D*: schematic representation of the H-reflex and the firing of single motor units (vertical lines).

stimulations of the tibial nerve at 5 mA intensity and increased every consecutive pulse for 1 mA. When the H-reflex amplitude started to decline, we increased the stimulation by 5 mA increments until the increase of the M-wave amplitude stopped rising (M_{MAX}).

To investigate the effects of the two interventions, we conditioned the H-reflex with nerve stimulations of homonymous spinal pathways to estimate the alterations in the level of presynaptic inhibition on Ia afferent terminals. Unconditioned H-reflexes functioned as a base for conditioned volleys arising from stimulation of the tibial nerve to elicit *1*) presynaptic inhibition ($D1_{P2P}$) (Fig. 1*C*). As suggested in the literature, 5 to 10 stimuli need to be elicited to achieve a reliable measure of the physiological response (19), and counteract the natural variability observed in H-reflex responses (28). At each time point, 15 unconditioned H-reflexes and 15 conditioned stimuli (30 stimuli total) were elicited in a pseudo-random order, without background muscle activity. To avoid the inhibitory effect of postactivation depression of the H-reflex, a quasi-random 10–12 s interstimulus interval was adopted (29). The assessment of the H-reflex started 15 s after the end of each intervention.

Unconditioned H-Reflex

To elicit the unconditioned SOL H-reflex, we stimulated the tibial nerve with a stimulation intensity that produced a response with H-reflex on the ascending part of the HM curve, anticipated by a visible M wave (M_{atH}) of amplitude between 5 and 10% of the maximal M_{MAX} (22). The quality of the stimulation was controlled with the reproducibility of the M_{atH} (30). The stability of M_{atH} ensured that the same number of motor units were stimulated by all stimuli (31). Hence, during the experiment, the intensity was adjusted to elicit a consistent M_{atH} amplitude. Real-time visual inspection of H-reflex was achieved by plotting 80-ms long intervals after each electrical stimulus using the biEMG LabChart software (32). The following parameters were extracted from each H-reflex: peak-to-peak amplitude (H_{P2P}); positive peak amplitude (H_{POS}); latency (H_{LAT}), representing the time

between the stimuli and the onset of the H-reflex; and duration (H_{DUR}), representing the time between the onset and end of the H-reflex. Parameters extracted from each H-reflex are graphically represented in Fig. 1*D*.

D1 Presynaptic Inhibition Assessment

To induce D1 presynaptic inhibition of Ia afferents, the H-reflexes were conditioned following the methodology presented by Knikou (22). Shortly, conditioning stimuli, comprising triple stimulations at 300 Hz (1-ms duration), were administered to the branch of the common peroneal nerve, activating the ipsilateral pretibial flexors using two surface electrodes made of silver chloride (8-mm diameter). These electrodes were positioned at the upper portion of the anterolateral side of the leg, distal to the caput fibulae. With the use of a Digitimer electrical stimulator (DS7R, Digitimer, Letchworth Garden City, UK), we delivered the electrical stimulation with an intensity of 1.2 times the motor threshold (MT) of the tibialis anterior (TA) (33). At the beginning of the session, the optimal timing between conditioning and test stimuli to achieve maximum H-reflex inhibition was determined for each participant. This procedure involved intervals between the stimulation of the tibial and common peroneal nerve ranging from 25 to 10 ms. Like the parameters extracted for the unconditioned H-reflex, the following parameters were extracted from the conditioned H-reflex: conditioned peak-to-peak amplitude ($D1_{P2P}$), conditioned positive peak amplitude ($D1_{POS}$), latency ($D1_{LAT}$), duration ($D1_{DUR}$). The activation of presynaptic inhibitory mechanisms was denoted by the difference between the unconditioned test response peak-to-peak amplitude (H_{P2P}) and the conditioned peak-to-peak response ($D1_{P2P}$) and calculated using the following formula (*Eq. 1*)

$$D1_{P2P} / H_{P2P}. \quad (1)$$

Equation 1: Formula used to calculate the ratio between conditioned and unconditioned H-reflex peak-to-peak amplitude, representing presynaptic inhibition.

Interventions

The first mobilization and relaxation intervention (exercise) consisted of stretching and coordination exercises targeting the orofacial, neck, and shoulder girdle muscles. These exercises focused on muscles that directly or indirectly participate in mastication and maintaining head posture (34, 35). The intervention protocol included 25 exercises: *exercises 1–4* were for tongue proprioception and control; *exercise 5* activated the orofacial muscle spindles and relaxed the orofacial muscles through desensitization; *exercise 6* was for facial muscle relaxation; *exercise 7* targeted relaxation of the mandible; *exercises 8* and *9* were mobilization exercises (held for 30 s, with a 10-s pause, repeated twice); *exercises 10–12* were coordination exercises (20 s active, with a 10-s pause, repeated three times); *exercises 13–16* were isometric strength exercises (held for 30 s, with a 10-s pause, repeated twice); *exercises 17* and *18* aimed to increase upper cervical flexion and extension; *exercises 19–24* were isometric exercises for the cervical region; and *exercise 25* was scapular retraction. *Exercises 17–25* also aimed to increase axial extension (cervical retraction). During the exercises and repetitions, subjects were asked to focus on breathing. The first intervention protocol lasted ~25 min.

The second intervention (chewing) comprised chewing a chunk of six commercially available chewing gums (~12 g) at a rate of 60 bites per minute for 6 min (36). No voluntary activation of the soleus was performed during any intervention. Additional details about the timings and repetitions of the exercises can be found in Table 1. Exercise pictures and video clips are available in the Supplemental Material Appendix I.

Data Analysis

All data presented in this study were collected with the HDsEMG electrode. Data analysis and cleaning were conducted in several steps: *1*) reflex extraction from HDsEMG, *2*) data cleaning, *3*) decomposition into MU, and *4*) MU firings extraction from reflex responses.

A detailed explanation of the methodology for detecting single motor units (MUs) firing during elicited contractions has been outlined in our previous studies (24, 25) and depicted in Fig. 2. Briefly, HDsEMG data underwent analysis using the Convolution Kernel Compensation (CKC) technique (37–39). Initially, data from the isometric force tracking procedure, acquired at the start of the experimental session, were decomposed for each contraction level (from 10% up to 70% MVC). The efficacy of decomposition was assessed quantitatively using the pulse-to-noise ratio (PNR), a reliable metric for MU identification precision (40). MUs with a PNR below 28 dB were excluded from subsequent analysis. The remaining MUs underwent meticulous scrutiny by an expert, with exclusions made for those displaying unusually low average firing rates (<8 Hz) or highly variable discharge patterns (coefficient of variation of interspike interval >0.4) (41). A specific MU filter was determined for each qualifying MU, representing the linear spatiotemporal combination of HDsEMG channels approximating the MU's spike train. Importantly, MU filters derived from one contraction were effectively applied to other contractions of the same muscle. Redundancies in MU identification across different voluntary contraction levels were rectified by retaining only the MU with the highest PNR if duplicates were identified (MUs sharing >30% of their firings with a firing match tolerance set to 0.25 ms). Refined MU filters were then applied to HDsEMG data from elicited H-reflexes, facilitating MU spike train identification. Categorization of identified MU spike train samples into actual firings or baseline noise was accomplished using threshold-based spike segmentation inherent to the CKC method. A manual review by an expert was conducted to verify the absence of cross talk in MU spike trains derived from both voluntary and elicited contractions, with manual adjustments made as needed.

MUs were categorized into three groups based on their recruitment threshold: $MU_{10–20}$, $MU_{30–40}$, $MU_{50–70}$, corresponding to detection during 10%–20%, 30%–40%, and 50%–70% of MVC force tracking tasks, respectively. The firing ratio ($MU_{fired/detected}$) was calculated by dividing the MUs that fired within a single elicited contraction by the total number of identified MUs in voluntary contractions for each participant. The MUs times of firing were defined as firing latencies (MU_{LAT}) and the standard deviation of latencies for

Table 1. *Details on exercise and chewing interventions*

Exercise *n*	Aim	Instructions
	Exercise intervention	
1	Tongue proprioception and control	Hold for 30 s. Rest for 10 s, repeat two times
2–4		Repeat at 0.5 Hz for 30 s. Rest for 10 s repeat for two times
5	Activate orofacial muscle spindles	Hold for 30 s. Rest for 10 s, repeat two times
6	Facial muscle relaxation	
7	Relaxation of the mandible	
8–9	Mobilization exercises	
10–12	Coordination exercises	Repeat at 0.5 Hz for 20 s. Rest for 10 s repeat for three times
13–18	Isometric strength exercises	Hold for 30 s. Rest for 10 s, repeat two times
19–24	Isometric exercises for the cervical region	Hold for 20 s. Rest for 10 s, repeat three times
25	Scapular retraction	
	Chewing intervention	
	Chewing	60 bites per minute for 6 min

each firing was calculated (MU_{SD}). MU_{LAT} and $MU_{fired/detected}$ were analyzed for all MUs and each MU threshold group, respectively.

To complement compound H-reflex measurements, PSTHs were constructed for individual motor units (MUs). For each MU, firings were extracted from high-density surface EMG recordings and binned into 0.25-ms epochs. PSTHs were generated separately for stimuli eliciting unconditioned and conditioned responses. The first 0.5 ms of the PSTH peak, corresponding to the monosynaptic Ia excitation window, was analyzed. Unconditioned firing counts within the first 0.5 ms from the onset of firing response of each MU was subtracted from the conditioned response and normalized to the number of stimuli. The computed metrics represents the D1 inhibition probability ($D1_{PROB}$), where larger negative values indicate stronger inhibition. Given the limited number of firings per MU, data were pooled across low-threshold MUs ($\leq$40% MVC) to construct population-level PSTHs per condition. This aggregation allowed for a more stable estimation of conditioned and unconditioned firing probabilities within the monosynaptic window. Consistent with evidence that presynaptic inhibition is more pronounced in low-threshold (slow) MUs (42), only units with recruitment thresholds $\leq$40% of maximal voluntary contraction (MVC) were included.

Statistical Analysis

Statistical analyses were performed in the R programming language (v.4.2.1) in the Rstudio environment (v.2022.07.1). To investigate the stability of stimulation, we calculated the individual M_{atH} coefficient of variation. To investigate the effects of experimental conditions (exercise, chewing) on various reflex outcomes for the maximal M-wave (M_{MAX}), H-reflex (H_{P2P}, H_{POS}, H_{LAT}, H_{DUR}), $D1_{P2P}$, and $D1_{P2P}/H_{P2P}$ response from the biEMG and from single MU analysis (MU_{LAT}, $MU_{fired/detected}$, MU_{SD}), we fitted linear mixed models ("*lmerTest*" package; 43) to predict values with intervention (exercise and chewing) and timepoint (PRE and POST) as fixed effects; formula: value $\sim$ intervention $\times$ timepoint. Interventions were set as random slope effects, whereas participants' ID and timepoints were used as nested random effects (formula: ~ 1 + intervention | DI) + (~ 1 | ID:time point). Model assumptions were checked using the performance package. Shortly, homogeneity of variance, low collinearity, normality of random effects, normality of residuals, and the absence of influential observations were visually inspected for each fitted model. To investigate the effects of intervention, timepoint, and MU firing threshold in the variables $MU_{fired/detected}$ and MU_{LAT}, we fitted a three-way linear mixed model with intervention (exercise and chewing) and timepoint (PRE and POST) and MU firing threshold (low, medium, high) as fixed effects; formula: value $\sim$ intervention $\times$ timepoint $\times$ MUthreshold, and participants ID as nested random effects (formula: $\sim 1|$ ID). $MU_{fired/detected}$ outcome variable is a ratio between fired and total detected MUs and $D1_{PROB}$, the inhibition probability computed using PSTHs from single MUs, is non-normally distributed, since it ranges on a scale between 0 and 1. Thus, we fitted a logistic mixed effect model (GLMM) in the "*glmmTMB*" package using a *beta* family distribution.

All the statistically significant effects were further analyzed by calculating the estimated marginal means in the "*emmeans*" package. The same package was used to calculate Cohen *d* effect sizes (as suggested by the package creators the sigma term has been enlarged by a factor of sqrt (2), to match the output of other software for paired data), between PRE and POST timepoints within each intervention and to calculate the interaction effect size. For data visualization, we used the "*ggplot2*" R package (44).

RESULTS

To provide a high-level orientation before presenting detailed statistical results, the main outcomes of the study are summarized later. A full account of all analyses, including model specifications and parameter estimates, follows in the subsequent sections. Overall, a reduction in H-reflex amplitude was observed exclusively following the exercise intervention. This effect was consistently reflected across multiple parameters, including H-reflex peak-to-peak amplitude (H_{P2P}), H-reflex positive peak amplitude (H_{POS}), and the $MU_{fired/detected}$ ratio. No significant modulation of background presynaptic inhibition was found in either intervention, as indicated by the $D1_{P2P}/H_{P2P}$ ratio derived from global EMG, and the $D1_{PROB}$ parameter extracted from PSTH analysis of single motor unit firings. In addition, H-reflex duration (H_{DUR}) was prolonged after exercise, whereas H-reflex latency (H_{LAT}) and motor unit firing latency (MU_{LAT}) remained unchanged, including when compared across recruitment thresholds. The variability of motor unit firing,

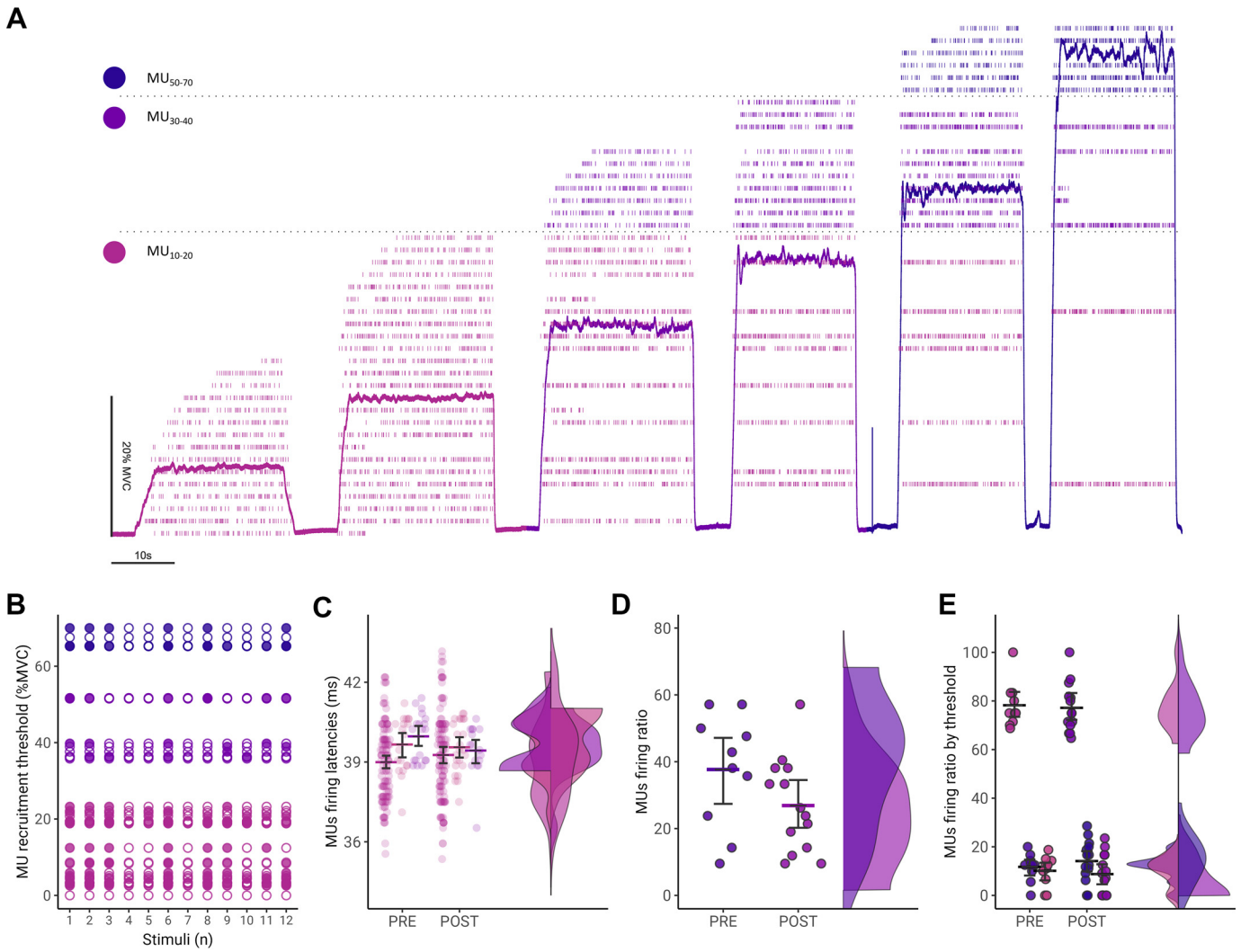

Figure 2. Representative data of a tested participant. *A*: identification of motor unit (MU) discharge patterns from high-density electromyography (HDsEMG) recorded during ramp contractions at 10%, 20%, 30%, 40%, 50%, and 70% maximum voluntary contraction (MVC). This procedure was used to define MU filters used to identify firings in elicited contractions. Three colors represent MU recruitment threshold clusters ($MU_{10–20}$, $MU_{30–40}$, $MU_{50–70}$). *B*: the detected MUs (empty dots) and fired MUs (filled dots) during different stimuli. *C*: comparison of MU firing latencies between $MU_{10–20}$, $MU_{30–40}$, $MU_{50–70}$ before and after the exercise intervention. *D*: comparison of MU firing ratio pre- and postexercise intervention. Each dot indicates the ratio of fired MU to all MUs for a single reflex for the subject. *E*: comparison of MU firing ratio by threshold cluster. Dots represent the ratio for $MU_{10–20}$, $MU_{30–40}$, $MU_{50–70}$ threshold groups before and after the exercise intervention. Estimated marginal mean values are depicted with horizontal lines, while the 95% confidence intervals are shown with shorter black lines. Kernel density estimation (density curves) of the data is displayed on the right as half-violin plots.

as assessed by motor unit firing standard deviation (MU_{SD}), showed no detectable changes.

Global EMG

Maximal and small M-wave amplitude and stability.

We first verified the stability of the stimulation across sessions. The analysis of the M_{MAX} of the time × intervention interaction was not statistically significant [$B = 0.04$, 95% confidence interval (CI) [−0.10, 0.18], $P = 0.571$; $\beta = 0.01$]. The coefficient of variability of the M_{atH} was 9.2% (SD = 5.5), which is usually interpreted as very good (45).

H-reflex peak-to-peak amplitude and positive peak amplitude.

We then examined the effects of the interventions on H-reflex amplitude characteristics. The analysis of the H_{P2P} revealed a significant time × intervention interaction [$B = 0.09$, 95% CI [0.07, 0.12], $t(644) = 7.06$, $P < 0.001$; $\beta = 0.56$]. Post hoc analysis revealed a significant reduction in H_{P2P} from PRE to POST in the exercise intervention ($P < 0.001$), whereas no significant change was observed in the chewing intervention ($P = 0.376$). Similarly, the analysis of the H_{POS} revealed a significant time × intervention interaction [$B = 0.08$, 95% CI [0.05, 0.11], $t(644) = 5.58$, $P < 0.001$; $\beta = 0.42$]. Post hoc analysis revealed a significant reduction in H_{POS} from PRE to POST in the exercise intervention ($P < 0.0001$), whereas the change in the chewing intervention was not significant ($P = 0.298$) (Fig. 3, *A* and *B*).

H-reflex latency and duration.

Next, we assessed latency and duration to explore potential changes in the temporal aspects of the H-reflex. The analysis

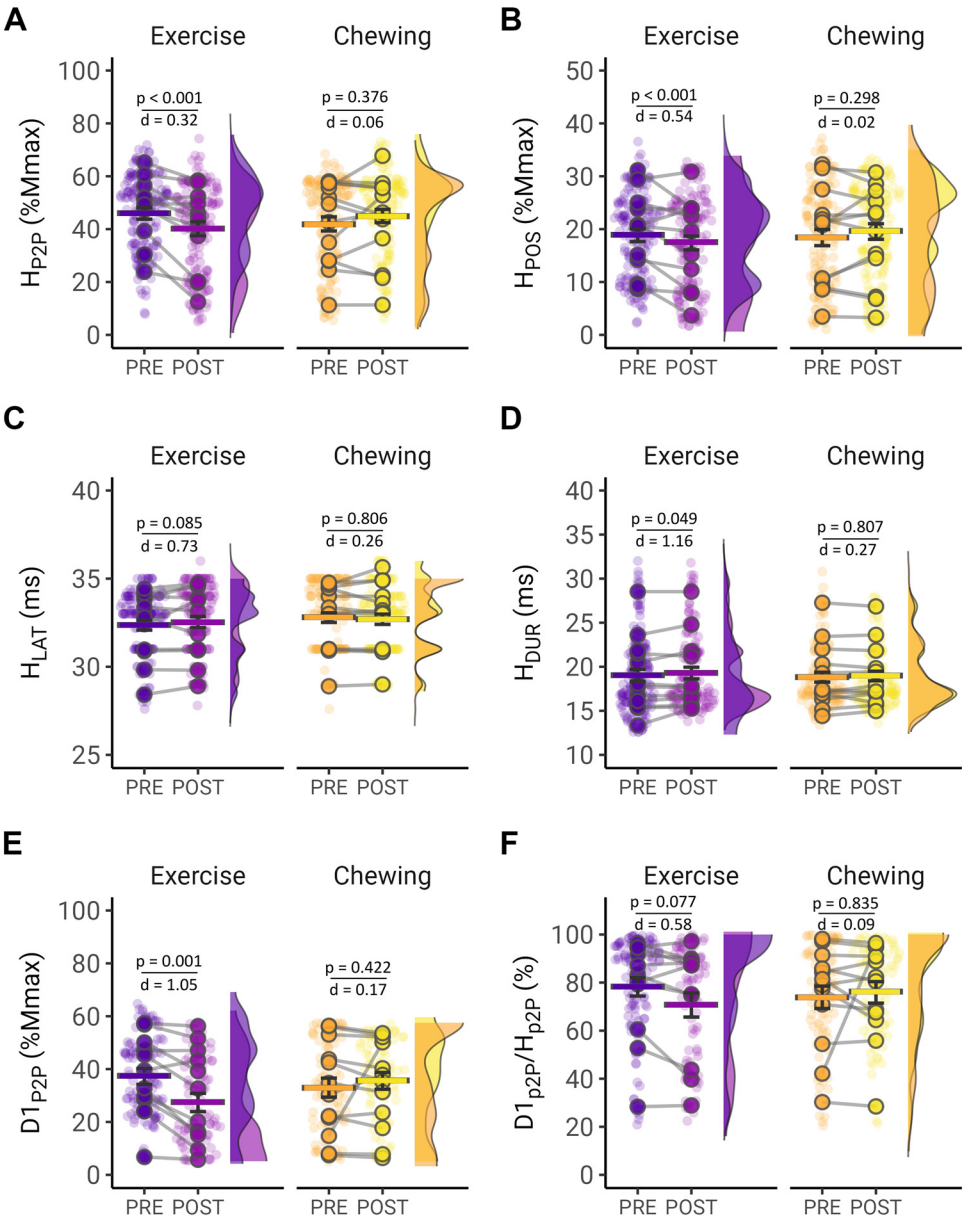

Figure 3. Data from global electromyography (EMG) pre- and postexercise and chewing interventions. *A*: Changes in H-reflex latency (H_{LAT}) before and after the exercise and chewing interventions. Blurred dots represent individual reflexes, and full dots represent the mean value for each participant. *B*: changes in H-reflex duration (H_{DUR}) before and after the interventions, with similar dot representation. *C*: changes in H-reflex positive peak amplitude (H_{POS}) comparing pre- and postintervention data. *D*: changes in H-reflex peak-to-peak amplitude (H_{P2P}) before and after the interventions. *E*: changes in $D1_{P2P}$ before and after the interventions. *F*: changes in $D1_{P2P}/H_{P2P}$ before and after the interventions. For all panels, estimated marginal mean values are depicted with bold horizontal colored lines, while 95% confidence intervals are shown with shorter black lines. Kernel density estimation (density curves) of the data is displayed on the right as half-violin plots, providing visual comparisons of the distributions.

of the H-reflex H_{LAT} revealed a significant time × intervention interaction [$B = -0.17$, 95% CI [−0.32, −0.01], $t(644) = -2.15$, $P = 0.032$; $\beta = -0.09$]. However, post hoc analysis indicated no significant changes in H_{LAT} from PRE to POST in the exercise intervention ($P = 0.085$), or in the chewing intervention ($P = 0.806$).

The analysis of the H-reflex H_{DUR} did not reveal any significant time × intervention interaction [$B = -0.32$, 95% CI [−0.67, 0.04], $t(644) = -1.76$, $P = 0.079$; $\beta = -0.08$]. The main effect of intervention revealed that the interventions had no significant effect on H_{DUR} [$B = -0.16$, 95% CI [−0.76, 0.45], $t(644) = -0.50$, $P = 0.617$; $\beta = -0.04$], and the main effect of time indicated a significant positive difference in H_{DUR} between pre and post data [$B = 0.36$, 95% CI [0.03, 0.69], $t(644) = 2.13$, $P = 0.034$; $\beta = 0.09$]. Post hoc analysis indicated a significant prolongation of H_{DUR} after the exercise intervention ($P = 0.049$) and no significant changes after the chewing intervention ($P = 0.807$) (Fig. 3, *C* and *D*).

D1 presynaptic inhibition.

To further probe spinal circuitry modulation, we analyzed the degree of presynaptic inhibition using the $D1_{P2P}$ ratio. In the analysis of the $D1_{P2P}$, a significant time × intervention interaction was observed [$B = 0.09$, 95% CI [0.06, 0.11], $t(372) = 6.72$; $P < 0.001$; $\beta = 0.52$]. Post hoc analysis indicated a significant decrease in $D1_{P2P}$ from PRE to POST in the exercise intervention ($P = 0.001$), whereas no significant change was observed in the chewing intervention ($P = 0.245$).

In the analysis of the $D1_{P2P}/H_{P2P}$, the time × intervention interaction was not statistically significant [$B = 0.04$, 95% CI [−0.01, 0.09], $t(373) = 1.42$, $P = 0.156$; $\beta = 0.17$]. The simple effect of the intervention indicated a nonsignificant difference in $D1_{P2P}/H_{P2P}$ between interventions [$B = -0.02$, 95% CI

[−0.07, 0.03], $t(373) = -0.80$, $P = 0.422$; $\beta = -0.09$], and the simple effect of time also showed a nonsignificant difference in $D1_{P2P}/H_{P2P}$ between pre and post data [$B = -0.03$, 95% CI [−0.07, 3.46*e*-03], $t(373) = -1.79$, $P = 0.075$; $\beta = -0.15$] (Fig. 3, *E* and *F*).

Per MU analysis.

Single motor unit (MU) analyses offered a more granular perspective on the reflex responses. A total of 376 motor units (MUs) were detected, with distribution across threshold categories as follows: 181, 115, and 80 for low, medium, and high threshold MUs, respectively. A total of 8,400 firings were observed in elicited conditions, with 4,501, 2,349, and 1,550 from low, medium, and high threshold MUs, respectively. Further details are provided in Table 2.

MUs firing latency.

We then examined changes in the firing latency of individual motor units across different thresholds. In the MU_{LAT} analysis of the unconditioned H-reflex, there was no significant time × intervention × threshold interaction ($B = -0.26$, 95% CI [−0.77, 0.24], $P = 0.302$; $\beta = -0.10$) for $MU_{10–20}$ versus $MU_{30–40}$ threshold MUs, and no interaction when confronting $MU_{10–20}$ to $MU_{50–70}$ threshold MUs ($B = 6.05e$-03, 95% CI [−0.56, 0.57], $P = 0.983$; $\beta = 2.37e$-03). A significant time × intervention interaction was observed ($B = -0.38$, 95% CI [−0.67, −0.09], $P = 0.010$; $\beta = -0.15$), a significant intervention × threshold interaction ($B = 0.42$, 95% CI [0.06, 0.78], $P = 0.022$; $\beta = 0.16$), and a time × threshold ($B = 0.51$, 95% CI [0.20, 0.82], $P = 0.001$; $\beta = 0.20$).

In the MU_{LAT} analysis of the conditioned H reflex, there was no significant time × intervention × threshold interaction [$B = -0.29$, 95% CI [−0.80, 0.22], $t(3,935) = -1.13$, $P = 0.260$; $\beta = -0.11$ $MU_{10–20}$ vs. $MU_{30–40}$ threshold MUs] and no interaction when comparing $MU_{10–20}$ to $MU_{50–70}$ threshold MUs [$B = 0.19$, 95% CI [−0.42, 0.80], $t(3,935) = 0.60$, $P = 0.552$; $\beta = 0.07$]. A significant time × intervention interaction was observed [$B = -0.61$, 95% CI [−0.91, −0.30], $t(3,935) = -3.94$, $P < 0.001$; $\beta = -0.23$], whereas a significant intervention × threshold interaction was found for $MU_{50–70}$ threshold MUs [$B = 0.59$, 95% CI [0.35, 0.84], $t(3,935) = 4.74$, $P < 0.001$; $\beta = 0.22$]. In addition, the time × threshold interaction was significant for $MU_{30–40}$ threshold MUs [$B = 0.48$, 95% CI [0.15, 0.81], $t(3,935) = 2.83$, $P = 0.005$; $\beta = 0.18$], but not for $MU_{50–70}$ threshold MUs [$B = -6.83e$-03, 95% CI [−0.42, 0.40], $t(3,935) = -0.03$, $P = 0.974$; $\beta = -2.58e$-03] (Fig. 4*A*).

Table 2. *Per MU summary statistics*

	n	Means ± SD
Detected MUs	376	37.60 ± 11.22
Low threshold MUs ($MU_{10–20}$)	181	18.10 ± 10.21
Medium threshold MUs ($MU_{30–40}$)	115	11.50 ± 3.34
High threshold MUs ($MU_{50–70}$)	80	8.00 ± 4.32
Total firings	8,400	840.00 ± 352.50
Low threshold MUs ($MU_{10–20}$)	4,501	450.10 ± 326.02
Medium threshold MUs ($MU_{30–40}$)	2,349	234.90 ± 109.58
High threshold MUs ($MU_{50–70}$)	1,550	155.00 ± 109.76
Firings per stimuli		7.97 ± 6.27
Low threshold MUs ($MU_{10–20}$)		4.74 ± 4.02
Medium threshold MUs ($MU_{30–40}$)		2.85 ± 2.29
High threshold MUs ($MU_{50–70}$)		2.37 ± 2.06

MUs, motor units; $MU_{10–20}$, low threshold motor units; $MU_{20–40}$, medium threshold motor units; $MU_{50–70}$, high threshold motor units; SD, standard deviation.

Reflex MUs ratio by recruitment threshold (three-way interaction).

To determine whether motor unit recruitment differed across conditions, we analyzed the ratio of fired to detected units across threshold groups. In the analysis of the unconditioned H-reflex for $MU_{fired/detected}$ no significant three-way interaction was observed between time × intervention × threshold ($B = -0.04$, 95% CI [−0.44, 0.37], $P = 0.866$; $\beta = -0.16$ for $MU_{10–20}$ vs. $MU_{30–40}$, and $B = -0.16$, 95% CI [−0.74, 0.41], $P = 0.579$; $\beta = -0.31$ for $MU_{10–20}$ vs. $MU_{50–70}$). In addition, no significant two-way interactions were found between time × intervention ($B = -1.07$, 95% CI [−1.38, −0.77], $P < 0.001$; $\beta = 0.39$), intervention × threshold ($B = 0.39$, 95% CI [−0.02, 0.81], $P = 0.062$; $\beta = -0.19$ for $MU_{10–20}$ vs. $MU_{30–40}$, and $B = -0.19$, 95% CI [−0.60, 0.23], $P = 0.375$; $\beta = -0.15$ for $MU_{10–20}$ vs. $MU_{50–70}$), or time × threshold ($B = -0.15$, 95% CI [−0.56, 0.26], $P = 0.473$; $\beta = 0.03$ for $MU_{10–20}$ vs. $MU_{30–40}$ and $B = 0.03$, 95% CI [−0.38, 0.44], $P = 0.878$; $\beta = -0.04$ for $MU_{10–20}$ vs. $MU_{50–70}$). Regarding simple effects, no significant effect of intervention was observed ($B = -0.31$, 95% CI [−0.88, 0.26], $P = 0.294$; $\beta = -0.10$), nor was there a significant effect of time ($B = -0.18$, 95% CI [−0.48, 0.12], $P = 0.239$; $\beta = -0.21$). However, significant simple effects were found for $MU_{50–70}$ ($B = -0.75$, 95% CI [−1.06, −0.45], $P < 0.001$; $\beta = -1.07$), whereas the effect for $MU_{30–40}$ was nonsignificant ($B = -0.21$, 95% CI [−0.51, 0.08], $P = 0.161$; $\beta = -0.75$).

In the analysis of the $D1_{P2P}$ conditioned H-reflex for $MU_{fired/detected}$, no significant three-way interaction was observed between time × intervention × threshold ($B = -0.34$, 95% CI [−0.76, 0.07], $P = 0.102$; $\beta = -0.17$ for $MU_{10–20}$ vs. $MU_{30–40}$, and $B = -0.17$, 95% CI [−0.76, 0.43], $P = 0.583$; $\beta = -0.02$ for $MU_{10–20}$ vs. $MU_{50–70}$). In addition, no significant two-way interactions were found between experiment × time ($B = -1.22$, 95% CI [−1.52, −0.91], $P < 0.001$; $\beta = 0.41$), intervention × threshold ($B = 0.41$, 95% CI [−0.02, 0.83], $P = 0.062$; $\beta = -0.02$ for $MU_{10–20}$ vs. $MU_{30–40}$, and $B = -0.02$, 95% CI [−0.44, 0.40], $P = 0.918$; $\beta = 0.10$ for $MU_{10–20}$ vs. $MU_{50–70}$), or time × threshold ($B = 0.10$, 95% CI [−0.31, 0.51], $P = 0.642$; $\beta = 0.15$ for $MU_{10–20}$ vs. $MU_{30–40}$, and $B = 0.15$, 95% CI [−0.27, 0.57], $P = 0.486$; $\beta = -0.34$ for $MU_{10–20}$ vs. $MU_{50–70}$). Regarding simple effects, no significant effect of intervention was observed [$B = -0.04$, 95% CI [−0.18, 0.10], $t(467) = -0.61$, $P = 0.545$; $\beta = -0.07$], nor was there a significant effect of time [$B = -0.07$, 95% CI [−0.22, 0.08], $t(467) = -0.88$, $P = 0.380$; $\beta = -0.11$]. However, significant simple effects were found for high threshold MUs ($B = -0.81$, 95% CI [−1.11, −0.51], $P < 0.001$; $\beta = -1.22$), whereas the effect for medium threshold MUs was nonsignificant ($B = -0.11$, 95% CI [−0.41, 0.19], $P = 0.481$; $\beta = -0.81$). In addition, the effect of time [POST] was statistically significant and negative ($B = -0.32$, 95% CI [−0.62, −0.02], $P = 0.037$; $\beta = -0.11$) (Fig. 4*B*).

Reflex MU firing ratio (two-way interaction).

We then analyzed the overall proportion of motor units that fired in response to the reflex stimulus without considering the MUs recruitment threshold. In the analysis of $MU_{fired/detected}$ for the unconditioned H-reflex, a

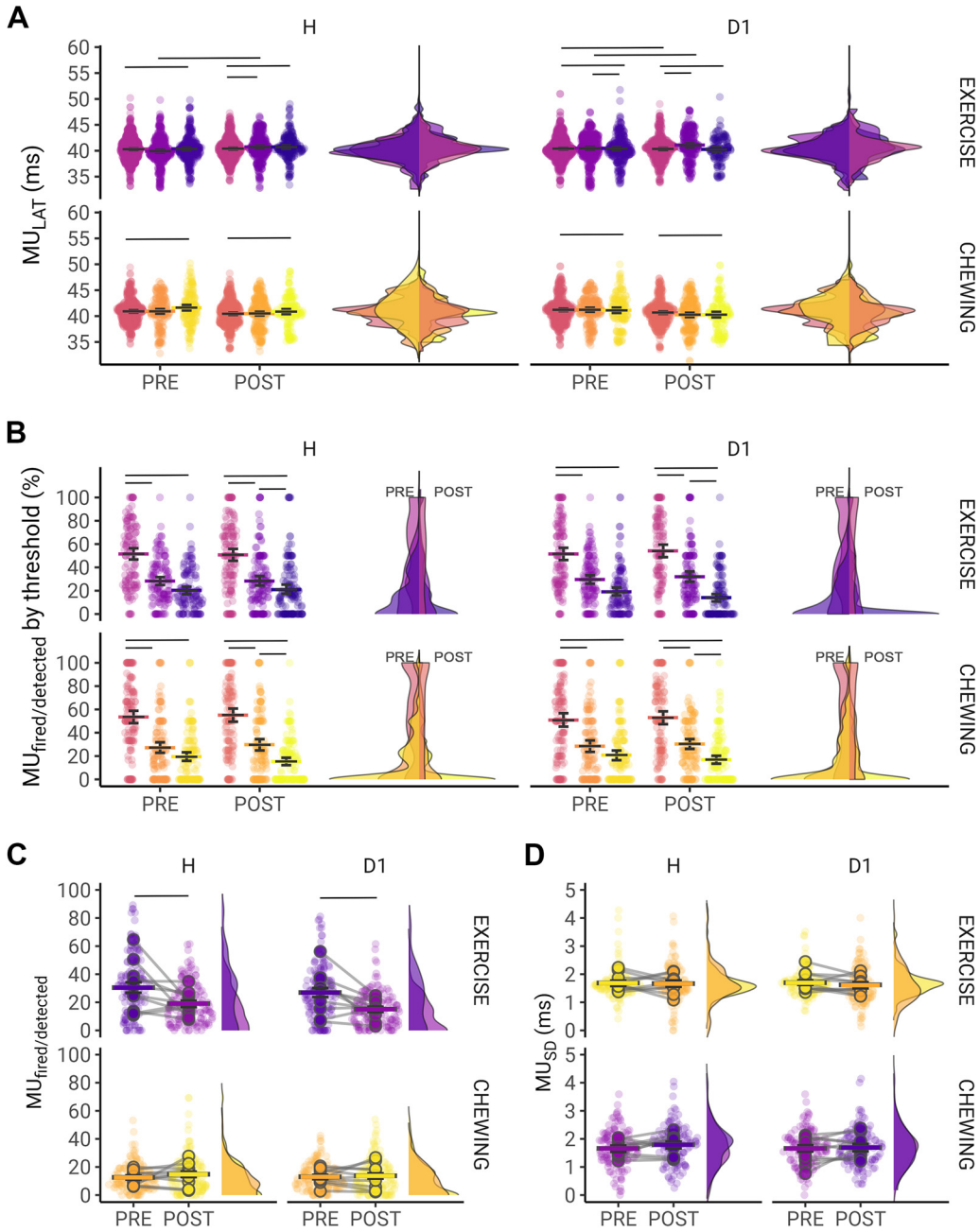

Figure 4. Data from single motor unit (MU) firings pre- and postexercise and chewing interventions decomposed from high-density electromyography (HDsEMG). *A*: changes in motor unit latency (MU_{LAT}) before and after the exercise and chewing interventions. Blurred dots represent individual firings. *B*: changes in $MU_{fired/detected}$ by threshold. *C*: changes in $MU_{fired/detected}$. *D*: changes in MU_{SD} comparing pre- and postintervention data. For all panels, estimated marginal mean values are depicted with bold horizontal colored lines, while 95% confidence intervals are shown with shorter black lines. Kernel density estimation (density curves) of the data is displayed on the right as half-violin plots, providing visual comparisons of the distributions. Statistically significant differences are indicated by horizontal lines.

significant interaction between the intervention × time was observed ($B = 0.73$, 95% CI [0.48, 0.99], $P < 0.001$; $\beta = 0.73$).

In the analysis of $MU_{fired/detected}$ for the conditioned H-reflex, a significant positive interaction between the intervention and time was observed ($B = 0.80$, 95% CI [0.55, 1.04], $P < 0.001$; $\beta = 0.80$). For simple effects, there was a significant effect of intervention ($B = -0.88$, 95% CI [−1.05, −0.71], $P < 0.001$; $\beta = -0.88$) and a significant effect of time ($B = -0.71$, 95% CI [−0.88, −0.55], $P < 0.001$; $\beta = -0.71$) (Fig. 4*C*).

MUs standard deviation.

Finally, we assessed the variability in MU firing using standard deviation as an index of response consistency. The analysis of the MU_{SD} for the unconditioned H-reflex revealed no significant interaction between the intervention and time [$B = 0.14$, 95% CI [−0.08, 0.35], $t(486) = 1.24$, $P = 0.215$; $\beta =$

0.21]. There was no significant simple effect of intervention [$B = -0.03$, 95% CI [−0.18, 0.12], $t(486) = -0.39$, $P = 0.696$; $\beta = -0.05$] and no significant simple effect of time [$B = -0.02$, 95% CI [−0.19, 0.15], $t(486) = -0.25$, $P = 0.800$; $\beta = -0.03$].

In the analysis of the $D1_{P2P}$ for the conditioned H-reflex for MU_{SD}, no significant interaction between the intervention and time was observed [$B = 0.10$, 95% CI [−0.10, 0.30], $t(467) = 1.00$, $P = 0.317$; $\beta = 0.17$]. There was no significant simple effect of intervention [$B = -0.04$, 95% CI [−0.18, 0.10], $t(467) = -0.61$, $P = 0.545$; $\beta = -0.07$] and no significant simple effect of time [$B = -0.07$, 95% CI [−0.22, 0.08], $t(467) = -0.88$, $P = 0.380$; $\beta = -0.11$] (Fig. 4*D*).

Post stimuli time histograms to infer D1 inhibition probability.

To further investigate the effects of the interventions on the presynaptic inhibition, we computed PSTHs to examine the inhibition probability of low- and medium-threshold MUs firings within the first 0.5 ms after the D1 conditioning stimulus ($D1_{PROB}$). The analysis revealed a significant main effect of intervention: the chewing condition was associated with higher firing probability compared with exercise ($B = 0.82$, 95% CI [0.23, 1.40], $P = 0.006$; $\beta = 0.82$). The main effect of time was not statistically significant ($B = 0.39$, 95% CI [−0.12, 0.90], $P = 0.130$; $\beta = 0.39$), nor was the time × intervention interaction ($B = -0.73$, 95% CI [−1.56, 0.09], $P = 0.082$; $\beta = -0.73$) (Fig. 5).

DISCUSSION

The aim of this study was to explore the effects of an upper body mobilization exercise protocol, and the impact of chewing, on the soleus H-reflex. In addition, we sought to identify consequential changes in MU discharge patterns of elicited contractions. Our findings revealed distinct responses at the global EMG level, represented by the decline of the H-reflex amplitude (H_{P2P}) and H-reflex positive peak (H_{POS}), accompanied by an increased reflex duration (H_{DUR}) following the exercise intervention while the

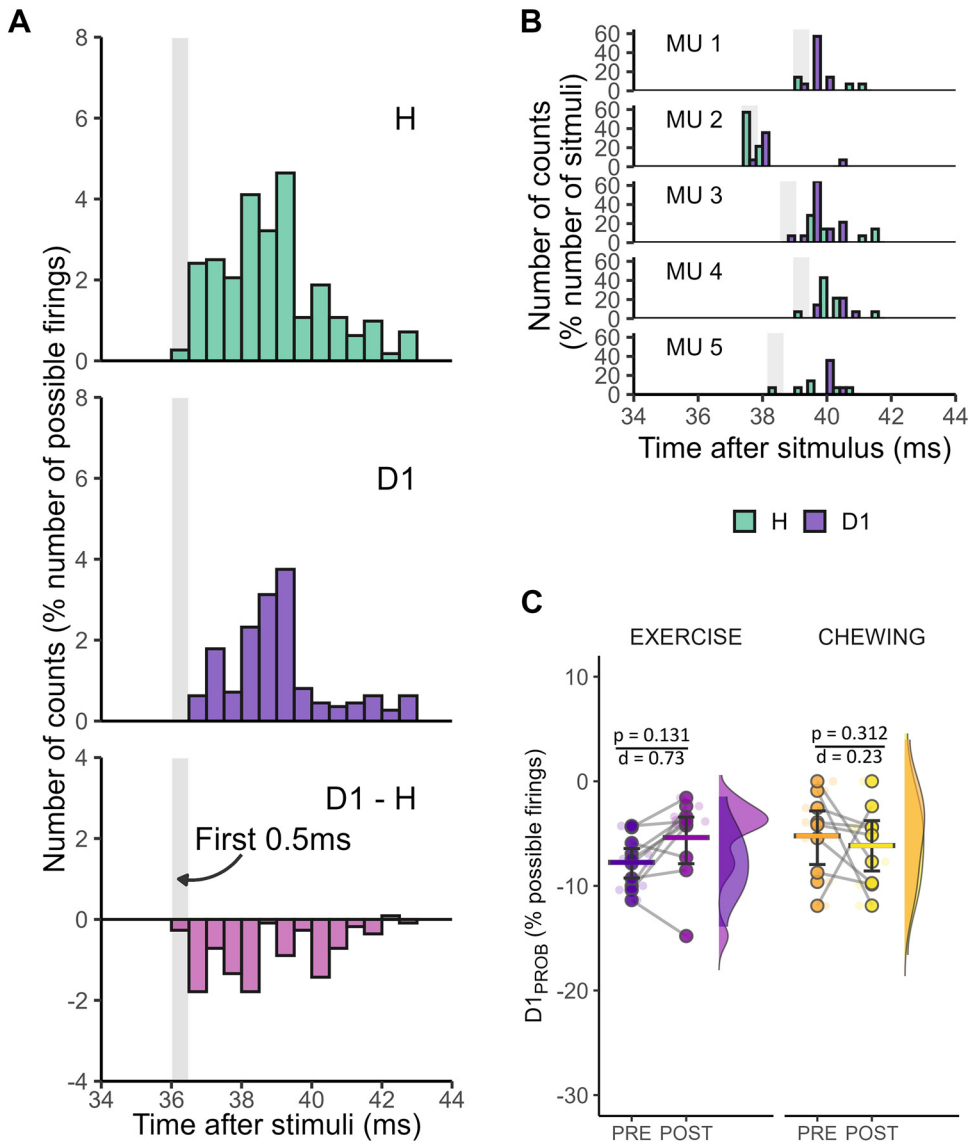

Figure 5. Data from single motor unit (MU) firings plotted as post stimuli time histograms (PSTH) in 0.5-ms bins. *A*: cumulative PSTH constructed from firings of MUs of a representative participant. Bin height reflects the total count of MU firings per epoch, normalized to the number of possible firings, calculated as (number of stimuli) × (number of detected MUs). *Top row*: unconditioned H-reflex firing probability (H). *Middle row*: D1-conditioned firing probability (D1). *Bottom row*: difference between D1 and H (D1 – H), where negative values indicate inhibition. The gray bar highlights the first 0.5-ms epoch. *B*: PSTHs for five MUs representing a subset of MUs used in *A*. To enable direct comparison of firing probabilities, unconditioned (green, H) and conditioned (purple, D1) firing probabilities are plotted side-by-side, with each bar representing values for the full duration of its respective 0.5-ms time bin. All depicted MUs are low-threshold MUs, recruited during voluntary contractions ≤20% maximum voluntary contraction (MVC). Despite shared recruitment thresholds, firing latency varied, confirming that single MU latency is not a reliable measure of recruitment order in elicited contractions extracted from HDsEMG. Gray bars represent the first 0.5-ms epoch of firing for each MU; data from this epoch were pooled across MUs and further analyzed. *C*: Changes in D1 inhibition firing probability ($D1_{PROB}$) before and after the exercise and chewing interventions. Estimated marginal mean values are depicted with bold horizontal-colored lines, while 95% confidence intervals are shown with shorter black lines. Kernel density estimation (density curves) of the data is displayed on the right as half-violin plots, providing visual comparisons of the distributions.

chewing intervention demonstrated negligible effects on these parameters. The divergence in responses between the two interventions underscores the nuanced modulation of the neural system in response to remote muscle relaxation (exercise) or contraction (chewing). Furthermore, analysis at the MU level revealed differential responses across MU discharge patterns, with a notable decrease detected in firing ratio after the exercise intervention, indicative of altered neuromuscular activity, which reinforces the findings at the global EMG level. Notably, the ratio between D1 and H-reflex peak-to-peak amplitude ($D1_{P2P}/H_{P2P}$) and the complementary analysis using PSTHs ($D1_{PROB}$), indicative of presynaptic inhibition mechanisms, was not affected by either intervention. These findings suggest that there is an intricate interplay between muscle contraction history on remote neural responses.

The observed decrease in H_{P2P} after the exercise intervention is not in line with previous studies investigating the remote effects of stretching on the H-reflex. For example, Anvar et al. (9) investigated the crossover soleus H-reflex responses to remote stretching on the contralateral limb and found that passive stretching (six times 45 s with a 15-s rest) did not cause significant changes in the M waves and H/M ratio. Similar results were reported by Coratella et al. (10) where stretching the contralateral plantar flexor up to 90% of maximal discomfort did not significantly interest the corticospinal activity. However, both aforementioned studies implied shorter stretching protocols compared with ours, making the comparison between studies challenging.

Similar to H_{P2P}, we observed a significant drop in H_{POS} after the exercise intervention. The positive peak of the H-reflex waveform was selected as a complementary parameter to traditional peak-to-peak amplitude, based on its electrophysiological relevance. Analogous to the M-wave, where the first (positive) phase reflects the propagation of action potentials along muscle fibers, while the second (negative) phase is influenced by nonpropagating extinction effects at the muscle fiber ends (end-of-fiber effect), the H-reflex positive peak likely offers a less biased reflection of spinal output (46). As such, H_{POS} may serve as a more specific marker of synchronized motoneuron discharge, independent of peripheral artifacts. Although prior studies have reported reductions in H-reflex amplitude under conditions of peripheral fatigue and ionic imbalance (47), these mechanisms are unlikely to apply here. All measurements were performed at rest, and the intervention involved remote orofacial musculature movement without direct or sustained activation of SOL. Therefore, peripheral mechanisms such as local metabolic fatigue or impaired conduction can be reasonably excluded.

Single MU analysis provided deeper insights into how the interventions affected MUs at different recruitment thresholds. In accordance with the literature, the most elicited MUs in H-reflexes were low-threshold (19), followed by middle- and high-threshold MUs. The firing ratio was significantly decreased after the exercise intervention uniformly across all three MU threshold categories (low-, middle-, and high-threshold MUs), which supports the observed drop in H_{P2P} registered in the global EMG analysis.

Although H_{LAT}, representing the latency of reflex onset, was not significantly affected, H_{DUR} was significantly longer after the exercise intervention, but not after the chewing intervention. An increase in H-reflex duration is often interpreted as a consequence of fatigue-induced slowing of action potential conduction velocity (48), particularly due to peripheral mechanisms such as metabolic changes in the muscle, resulting in a changed MUAP shape. However, in the present study, the soleus was not voluntarily activated during either intervention, or activation occurred only through electrical stimulation. As the number of stimuli was identical across all time points (30 stimuli pre- and postintervention), it is unlikely that the observed prolongation of H_{DUR} resulted from peripheral fatigue only in a single intervention. Instead, we propose that the longer H_{DUR} observed in this study could reflect central mechanisms such as changes in recruitment of lower- and higher-threshold MUs or a reduced temporal synchronization of MU firings within the motoneuron pool. These central processes would result in more dispersed MU discharge timing, thereby extending the duration of the compound response, affecting also the amplitude of the compound H-reflex. Although the standard deviation of MU firing latencies within each reflex response did not significantly differ between conditions, suggesting stable synchronization, this measure may not fully capture subtle shifts in temporal recruitment dispersion. Moreover, no significant differences were observed in the standard deviation or between firing ratios of different MU thresholds, suggesting that spinal mechanisms causing the drop in H_{P2P} after the exercise intervention uniformly affect the motoneuron pool (19).

Many possible mechanisms could cause the observed drop in H_{P2P} after the exercise intervention. Modulation of the final motor output can occur by ionotropic or neuromodulatory inputs. Ionotropic modulation may involve pre- and/or postsynaptic mechanisms (49). It has been suggested that a decrease in H-reflex amplitude following similar interventions could be attributed to increased presynaptic inhibition (50). In our study, although a significant decrease in the $D1_{P2P}$ parameter (derived from global EMG recordings) was observed after the exercise intervention, the $D1_{P2P}/H_{P2P}$ ratio remained unchanged. In addition, the $D1_{PROB}$ metric extracted from PSTH analysis of single MUs, arguably a more direct indicator of monosynaptic Ia presynaptic inhibition, also showed no significant differences between pre- and postintervention. These findings suggest that presynaptic inhibition, as assessed via D1 metrics, may not fully account for the observed reduction in H_{P2P}.

To better understand this discrepancy, we considered recent work that has re-evaluated the traditional models of presynaptic inhibition and explored additional spinal mechanisms that could underlie reflex modulation. Presynaptic inhibition has traditionally been attributed to the activation of $GABA_A$ receptors on Ia afferent terminals by PAD interneurons (51). However, recent evidence suggests that $GABA_A$ receptors are not predominantly located on the Ia terminals themselves, but rather near nodes of Ranvier along the afferent axon. At these nodal sites, $GABA_A$ receptor activation facilitates spike propagation rather than inhibiting it (52). Therefore, the classical PAD mechanism involving $GABA_A$ receptors may not directly account for presynaptic inhibition at the Ia-motoneuron synapse. Instead, it has been proposed that $GABA_A$-mediated PAD can trigger orthodromic

spikes in the Ia afferents, which in turn produce postactivation depression, a form of presynaptic inhibition driven by reduced neurotransmitter release and potentially modulated by $GABA_B$ receptor activity at the Ia afferent terminals (53). In addition, Budini et al. (54) reported two phases of H-reflex inhibition, a presynaptic postactivation depression of Ia afferent, and a weaker postactivation depression from secondary afferents. These newer interpretations challenge long-held assumptions and suggest that multiple temporally layered mechanisms may underlie reflex suppression. Although our experimental design did not allow us to isolate these specific mechanisms, their involvement may help explain the absence of significant effects in conventional D1 metrics in our study.

In addition to presynaptic modulation, it is possible that the observed reduction in H_{P2P} following the exercise protocol was influenced by postsynaptic or descending supraspinal inputs. Several descending tracts, including corticospinal, rubrospinal, and vestibulospinal pathways, can influence spinal excitability and reflex modulation through both direct and indirect inputs onto spinal interneurons. For instance, increased Ia reciprocal inhibition, potentially influenced by descending inputs such as those from the corticospinal tract, could have contributed to the observed reflex suppression (22). In addition, projections from Ia afferents to the sensorimotor cortex may transform the descending corticospinal output and modulate reflex excitability at the spinal level (55). Postsynaptic inhibitory mechanisms may also include enhanced Ib inhibition mediated by Golgi tendon organs or recurrent inhibition via Renshaw cells (22, 56). Furthermore, exteroceptive reflexes arising from cutaneous receptor activation can transiently reduce sympathetic excitation and motoneuron output (49); however, this effect is short-lasting and unlikely to have contributed meaningfully to the postintervention changes observed in our study (57). Disfacilitation due to reduced excitatory input from type I and II muscle spindle afferent cortical projections might also play a role in the observed modulation of H_{P2P} (49, 58).

Another possible mechanism contributing to the observed reduction in H_{P2P} is the involvement of the neuromodulatory system, which influences the intrinsic excitability of motoneurons (59). Although we did not directly assess neuromodulatory influences, previous studies suggest that decreased excitability of the spinal reflex loop may result from a reduction in the strength of persistent inward currents (PICs) (60–62). PICs amplify and prolong synaptic inputs to motoneurons, and their strength depends on the activity of monoaminergic systems, which modulate the flow of positively charged ions into the cell membrane (63). A reduction in PIC activity leads to enhanced after-hyperpolarization, decreasing the likelihood of motoneuron firing in response to synaptic input. This has been supported by studies such as Mesquita et al. (61) who found that a whole body relaxation intervention (e.g., listening to soothing piano music) reduced estimated PIC strength and motoneuron excitability. Although speculative in the context of our findings, this pathway may offer an additional explanation for the reduced reflex amplitude following the exercise intervention.

In contrast to the exercise intervention, no significant changes were observed in any H-reflex parameters following the chewing protocol. This finding appears inconsistent with several studies reporting facilitation of the soleus H-reflex during oral motor activity, particularly during teeth clenching. For example, it has been shown that teeth clenching can facilitate the H-reflex amplitude even under fatigued conditions, with the amplitude increasing proportionally to bite force (5, 64, 65). Although the mechanisms underlying these effects are not fully understood, potential contributors include proprioceptive input from oral tissues, masticatory muscles, and temporomandibular joint (66). Moreover, Boroojerdi et al. (2) used transcranial magnetic stimulation and observed subcortical facilitation near the foramen magnum during teeth clenching, which coincided with enhanced H-reflex amplitude, suggesting modulation at subcortical levels. Furthermore, Mesquita et al. (67) proposed that jaw clenching may increase PIC activity, thus enhancing intrinsic motoneuron excitability (67).

However, research specifically investigating the acute effects of chewing, as opposed to forceful clenching, is limited. Takahashi et al. (15) reported that mastication enhances the SOL H-reflex amplitude during the chewing activity itself, without clear phase-dependent modulation. They attributed this effect to tonic, nonreciprocal facilitation of the lower-limb motoneuron pool, potentially driven by spindle afferents from the jaw-closing muscles (15, 65). Similarly, Hagiya (16) suggested that descending input from the pontobulbar reticular formation during rhythmic mastication may contribute to increased H-reflex excitability. In addition, an increase in H-reflex amplitude of both plantarflexor and dorsiflexor muscles during mastication has been reported (16), possibly reflecting an overall enhancement of spinal motoneuron excitability. These effects may result from a decrease in Ia presynaptic inhibition, allowing greater Ia afferent contribution to the motoneuron pool (19). However, no modulation in any electrophysiological parameter was observed in the present study following the chewing intervention. This discrepancy may be explained by differences in study design. Previous investigations have typically assessed H-reflex modulation during chewing or clenching tasks, with participants instructed to exert maximal or submaximal bite force (2, 5, 64, 68). In contrast, in our study, reflex measurements were performed after the chewing had ceased, with the first H-reflex elicited 15 s following the end of the chewing intervention. Although this timing was selected to capture acute effects, prior work suggests that the facilitation of the H-reflex induced by jaw activity dissipates rapidly once the behavior stops, often within a few seconds (15, 64). Therefore, the discrepancy between our findings and earlier studies is likely attributable to the delayed timing of postintervention measurements, which may have missed the short-lived window of spinal facilitation observed during active chewing or teeth clenching.

Nevertheless, our primary aim was not to measure reflex modulation during chewing itself (with already known effects), but to explore whether a brief bout of chewing could induce acute remote neural facilitation with potential therapeutic relevance. From this perspective, the absence of H-reflex modulation postchewing provides valuable information: it suggests that the neural consequences of rhythmic mastication may be short-lived and may not persist beyond the activity. Future studies should clarify whether repeated

or prolonged chewing interventions, or alternate timing protocols, can elicit more sustained effects on spinal excitability.

This study has several limitations. First, due to technical constraints, we could not assess heteronymous Ia facilitation, a critical method for corroborating presynaptic inhibition. This omission limits our ability to conclusively attribute H-reflex changes to presynaptic mechanisms, as alternative spinal pathways (e.g., postsynaptic inhibition) cannot be fully excluded (30). Second, our sample comprised only healthy individuals, restricting generalizability to populations with cervical or neuromuscular disorders. However, this aligns with our focus on exploring acute remote effects in neurotypical adults. Third, all measurements were conducted at rest, permitting only a single response per motor unit (MU) and precluding the use of peristimulus frequencygrams (PSFs), which require sustained firing patterns. The PSTH analysis, while informative, carries inherent methodological constraints. Traditional PSTH protocols rely on hundreds of stimuli to ensure statistical robustness, whereas we applied only 30 stimuli per condition (15 unconditioned, 15 conditioned). This limited stimulus count resulted in sparse firing distributions per bin, reducing reliability at the single-MU level. To compensate, we aggregated data across MUs, a necessary but imperfect solution, as it assumes physiological homogeneity across MUs. Furthermore, MU recruitment during electrically elicited H-reflexes, as recorded via high-density surface EMG (HDsEMG), may not strictly follow the size principle. As described by Škarabot et al. (25), the observed discrepancy between recruitment threshold during voluntary contractions and firing latency during elicited contractions does not reflect a physiological characteristic, but rather a methodological artifact. In their study, the authors conducted simulations to demonstrate that highly synchronized depolarization of the α-motoneuron pool via Ia afferents during electrically elicited contractions compresses latency differences between low- and high-threshold MUs. This effect, combined with faster conduction velocities and variable innervation zones of individual MUs, risks conflating recruitment thresholds with latency shifts. To mitigate this, we aggregated data across MUs and excluded high-threshold units. However, residual confounding remains possible. Future interventional studies should incorporate low-intensity background muscle activity to circumvent postactivation depression (a common limitation in resting H-reflex paradigms) and enable a higher number of stimuli within a similar assessment time window. This approach would enhance the robustness of the adopted noninvasive methodology, increasing the insights into spinal mechanisms provided by PSTH/PSF analysis. In addition, the chewing and stretching interventions were not applied under tightly controlled conditions, particularly in terms of chewing intensity and duration, which may have introduced variability. These interventions are based on distinct physiological mechanisms and were not designed to be directly compared or counteract one another. Our goal was to explore their individual capacity to modulate neuromuscular excitability. Future studies should implement more rigorously controlled protocols to better isolate the effects of chewing tasks. Finally, our findings reflect acute effects; thus, long-term adaptations remain unexplored.

Significance

The exercise protocol targeting orofacial and neck muscles resulted in an acute remote decrease in soleus H-reflex amplitude. Although the exact mechanisms remain uncertain, the observed modulation may involve a combination of spinal processes, though our findings suggest presynaptic inhibition is unlikely to be the primary contributor. By applying advanced signal processing to high-density surface EMG (HDsEMG) recordings, including the construction of peristimulus time histograms (PSTHs), we extracted single motor unit (MU) discharge behavior during elicited contractions, providing deeper physiological insight and complementing traditional global H-reflex metrics.

These findings highlight the potential application of orofacial and neck mobility exercises as a nonpharmacological strategy for modulating spinal excitability. Such interventions may hold promise for managing conditions associated with motoneuron hyperexcitability or for promoting general relaxation and rehabilitation. However, caution is warranted in generalizing these results to clinical populations. The present study involved only healthy individuals, and future research should investigate both the acute and long-term effects of these interventions in specific patient subgroups to clarify their therapeutic potential and limitations.

DATA AVAILABILITY

Data will be made available upon reasonable request.

SUPPLEMENTAL MATERIAL

Supplemental Material Appendix I: https://doi.org/10.17605/OSF.IO/U7JYV.

GRANTS

A.H., M. Kramberger, and N.M. were supported by the European Union's Horizon Europe Research and Innovation Program HybridNeuro project, GA No. 101079392 and by the Slovenian Research and Innovation Agency Programme P2-0041. Views and opinions expressed are however those of the author(s) only and do not necessarily reflect those of the European Union or Research Executive Agency. Neither the European Union nor the granting authority can be held responsible for them.

DISCLOSURES

No conflicts of interest, financial or otherwise, are declared by the authors.

AUTHOR CONTRIBUTIONS

M.M., A.H., M. Kramberger, M.V., A.F., and M. Kalc conceived and designed research; M.M., A.H., M. Kramberger, M.V., N.M., and M. Kalc performed experiments; M.M., A.H., M. Kramberger, M.V., N.M., and M. Kalc analyzed data; M.M., A.H., M. Kramberger, and M. Kalc interpreted results of experiments; A.H. and M. Kalc prepared figures; M.M. and M. Kalc drafted manuscript; M.M., A.H., M. Kramberger, M.V., A.F., and M. Kalc edited and revised manuscript; M.M., A.H., M. Kramberger, M.V., N.M., A.F., and M. Kalc approved final version of manuscript.

REFERENCES

1. **Ertuglu LA**, **Karacan I**, **Yilmaz G**, **Türker KS.** Standardization of the Jendrassik maneuver in Achilles tendon tap reflex. *Clin Neurophysiol Pract* 3: 1–5, 2018. doi:10.1016/j.cnp.2017.10.003.
2. **Boroojerdi B**, **Battaglia F**, **Muellbacher W**, **Cohen LG.** Voluntary teeth clenching facilitates human motor system excitability. *Clin Neurophysiol* 111: 988–993, 2000. doi:10.1016/s1388-2457(00)00279-0.
3. **Kawakubo N**, **Miyamoto JJ**, **Katsuyama N**, **Ono T**, **Honda E-I**, **Kurabayashi T**, **Taira M**, **Moriyama K.** Effects of cortical activations on enhancement of handgrip force during teeth clenching: an fMRI study. *Neurosci Res* 79: 67–75, 2014. doi:10.1016/j.neures.2013.11.006.
4. **Iida T**, **Kato M**, **Komiyama O**, **Suzuki H**, **Asano T**, **Kuroki T**, **Kaneda T**, **Svensson P**, **Kawara M.** Comparison of cerebral activity during teeth clenching and fist clenching: a functional magnetic resonance imaging study. *Eur J Oral Sci* 118: 635–641, 2010. doi:10.1111/j.1600-0722.2010.00784.x.
5. **Tanrıverdi U**, **Gündüz A**, **Hatice Kumru N**, **Kızıltan ME.** Cutaneous silent period modulation by tooth clenching, tonic and phasic limb movements in healthy subjects. *Exp Brain Res* 240: 2783–2789, 2022. doi:10.1007/s00221-022-06455-y.
6. **Mitsuyama A**, **Takahashi T**, **Ueno T.** Effects of teeth clenching on the soleus H reflex during lower limb muscle fatigue. *J Prosthodont Res* 61: 202–209, 2017. doi:10.1016/j.jpor.2016.05.003.
7. **Rossi-Durand C.** The influence of increased muscle spindle sensitivity on Achilles tendon jerk and H-reflex in relaxed human subjects. *Somatosens Mot Res* 19: 286–295, 2002. doi:10.1080/0899022021000037755.
8. **Dowman R**, **Wolpaw JR.** Jendrassik maneuver facilitates soleus H-reflex without change in average soleus motoneuron pool membrane potential. *Exp Neurol* 101: 288–302, 1988. doi:10.1016/0014-4886(88)90012-x.
9. **Anvar SH**, **Granacher U**, **Konrad A**, **Alizadeh S**, **Culleton R**, **Edwards C**, **Goudini R**, **Behm DG.** Corticospinal excitability and reflex modulation in a contralateral non-stretched muscle following unilateral stretching. *Eur J Appl Physiol* 123: 1837–1850, 2023. doi:10.1007/s00421-023-05200-9.
10. **Coratella G**, **Cè E**, **Doria C**, **Borrelli M**, **Longo S**, **Esposito F.** Neuromuscular correlates of the contralateral stretch-induced strength loss. *Med Sci Sports Exerc* 53: 2066–2075, 2021. doi:10.1249/MSS.0000000000002677.
11. **Pulverenti TS**, **Trajano GS**, **Kirk BJC**, **Blazevich AJ.** The loss of muscle force production after muscle stretching is not accompanied by altered corticospinal excitability. *Eur J Appl Physiol* 119: 2287–2299, 2019. doi:10.1007/s00421-019-04212-8.
12. **Pulverenti TS**, **Trajano GS**, **Walsh A**, **Kirk BJC**, **Blazevich AJ.** Lack of cortical or Ia-afferent spinal pathway involvement in muscle force loss after passive static stretching. *J Neurophysiol* 123: 1896–1906, 2020. doi:10.1152/jn.00578.2019.
13. **Masugi Y**, **Obata H**, **Inoue D**, **Kawashima N**, **Nakazawa K.** Neural effects of muscle stretching on the spinal reflexes in multiple lower-limb muscles. *PLoS One* 12: e0180275, 2017. doi:10.1371/journal.pone.0180275.
14. **Cè E**, **Coratella G**, **Bisconti AV**, **Venturelli M**, **Limonta E**, **Doria C**, **Rampichini S**, **Longo S**, **Esposito F.** Neuromuscular versus mechanical stretch-induced changes in contralateral versus ipsilateral muscle. *Med Sci Sports Exerc* 52: 1294–1306, 2020. doi:10.1249/MSS.0000000000002255.
15. **Takahashi T**, **Ueno T**, **Taniguchi H**, **Ohyama T**, **Nakamura Y.** Modulation of H reflex of pretibial and soleus muscles during mastication in humans. *Muscle Nerve* 24: 1142–1148, 2001. doi:10.1002/mus.1125.
16. **Hagiya N.** [Modulation of spinal monosynaptic reflexes during rhythmical jaw movements and its central neural mechanisms]. *Kokubyo Gakkai Zasshi* 61: 21–38, 1994. doi:10.5357/koubyou.61.21.
17. **Kang H-S**, **Kwon H-W**, **Kim D-G**, **Park K-R**, **Hahm S-C**, **Park J-H.** Effects of the suboccipital muscle inhibition technique on the range of motion of the ankle joint and balance according to its application duration: a randomized controlled trial. *Healthcare (Basel)* 9: 646, 2021. doi:10.3390/healthcare9060646.
18. **McNeil CJ**, **Butler JE**, **Taylor JL**, **Gandevia SC.** Testing the excitability of human motoneurons. *Front Hum Neurosci* 7: 152, 2013. doi:10.3389/fnhum.2013.00152.
19. **Theodosiadou A**, **Henry M**, **Duchateau J**, **Baudry S.** Revisiting the use of Hoffmann reflex in motor control research on humans. *Eur J Appl Physiol* 123: 695–710, 2023. doi:10.1007/s00421-022-05119-7.
20. **Pierrot-Deseilligny E**, **Burke D.** *The Circuitry of the Human Spinal Cord: Its Role in Motor Control and Movement Disorders—Presynaptic Inhibition* (1st ed.). 2005. Cambridge University Press.
21. **Knikou M.** Neural coupling between the upper and lower limbs in humans. *Neurosci Lett* 416: 138–143, 2007. doi:10.1016/j.neulet.2007.01.072.
22. **Knikou M.** The H-reflex as a probe: pathways and pitfalls. *J Neurosci Methods* 171: 1–12, 2008. doi:10.1016/j.jneumeth.2008.02.012.
23. **Hultborn H**, **Meunier S**, **Morin C**, **Pierrot-Deseilligny E.** Assessing changes in presynaptic inhibition of I a fibres: a study in man and the cat. *J Physiol* 389: 729–756, 1987. doi:10.1113/jphysiol.1987.sp016680.
24. **Kalc M**, **Skarabot J**, **Divjak M**, **Urh F**, **Kramberger M**, **Vogrin M**, **Holobar A.** Identification of motor unit firings in H-reflex of soleus muscle recorded by high-density surface electromyography. *IEEE Trans Neural Syst Rehabil Eng* 31: 119–129, 2023. doi:10.1109/TNSRE.2022.3217450.
25. **Škarabot J**, **Ammann C**, **Balshaw TG**, **Divjak M**, **Urh F**, **Murks N**, **Foffani G**, **Holobar A.** Decoding firings of a large population of human motor units from high-density surface electromyogram in response to transcranial magnetic stimulation. *J Physiol* 601: 1719–1744, 2023. doi:10.1113/JP284043.
26. **Botter A**, **Vieira TM.** Optimization of surface electrodes location for H-reflex recordings in soleus muscle. *J Electromyogr Kinesiol* 34: 14–23, 2017. doi:10.1016/j.jelekin.2017.03.003.
27. **Hermens HJ**, **Freriks B**, **Disselhorst-Klug C**, **Rau G.** Development of recommendations for SEMG sensors and sensor placement procedures. *J Electromyogr Kinesiol* 10: 361–374, 2000. doi:10.1016/s1050-6411(00)00027-4.
28. **Gossard JP**, **Floeter MK**, **Kawai Y**, **Burke RE**, **Chang T**, **Schiff SJ.** Fluctuations of excitability in the monosynaptic reflex pathway to lumbar motoneurons in the cat. *J Neurophysiol* 72: 1227–1239, 1994. doi:10.1152/jn.1994.72.3.1227.
29. **Burke D.** Clinical uses of H reflexes of upper and lower limb muscles. *Clin Neurophysiol Pract* 1: 9–17, 2016. doi:10.1016/j.cnp.2016.02.003.
30. **Pierrot-Deseilligny E**, **Mazevet D.** The monosynaptic reflex: a tool to investigate motor control in humans. Interest and limits. *Neurophysiol Clin* 30: 67–80, 2000. doi:10.1016/s0987-7053(00)00062-9.
31. **Crone C**, **Hultborn H**, **Mazières L**, **Morin C**, **Nielsen J**, **Pierrot-Deseilligny E.** Sensitivity of monosynaptic test reflexes to facilitation and inhibition as a function of the test reflex size: a study in man and the cat. *Exp Brain Res* 81: 35–45, 1990. doi:10.1007/BF00230098.
32. **Zehr EP.** Considerations for use of the Hoffmann reflex in exercise studies. *Eur J Appl Physiol* 86: 455–468, 2002. doi:10.1007/s00421-002-0577-5.
33. **Achache V**, **Roche N**, **Lamy J-C**, **Boakye M**, **Lackmy A**, **Gastal A**, **Quentin V**, **Katz R.** Transmission within several spinal pathways in adults with cerebral palsy. *Brain* 133: 1470–1483, 2010. doi:10.1093/brain/awq053.
34. **Moraes A da R**, **Sanches ML**, **Ribeiro EC**, **Guimarães AS.** Therapeutic exercises for the control of temporomandibular disorders. *Dental Press J Orthod* 18: 134–139, 2013. doi:10.1590/s2176-94512013000500022.
35. **Kisner C**, **Colby LA**, **Borstad J.** *Therapeutic Exercise: Foundations and Techniques*. F.A. Davis, 2017.
36. **Song C**, **Yu Y-F**, **Ding W-L**, **Yu J-Y**, **Song L**, **Feng Y-N**, **Zhang Z-J.** Quantification of the masseter muscle hardness of stroke patients using the MyotonPRO apparatus: intra- and inter-rater reliability and its correlation with masticatory performance. *Med Sci Monit* 27: e928109, 2021. doi:10.12659/MSM.928109.
37. **Negro F**, **Muceli S**, **Castronovo AM**, **Holobar A**, **Farina D.** Multi-channel intramuscular and surface EMG decomposition by convolutive blind source separation. *J Neural Eng* 13: 026027, 2016. doi:10.1088/1741-2560/13/2/026027.
38. **Holobar A**, **Farina D**, **Gazzoni M**, **Merletti R**, **Zazula D.** Estimating motor unit discharge patterns from high-density surface electromyogram. *Clin Neurophysiol* 120: 551–562, 2009. doi:10.1016/j.clinph.2008.10.160.
39. **Holobar A**, **Minetto MA**, **Botter A**, **Negro F**, **Farina D.** Experimental analysis of accuracy in the identification of motor unit spike trains

from high-density surface EMG. *IEEE Trans Neural Syst Rehabil Eng* 18: 221–229, 2010. doi:10.1109/TNSRE.2010.2041593.
40. **Holobar A**, **Minetto MA**, **Farina D.** Accurate identification of motor unit discharge patterns from high-density surface EMG and validation with a novel signal-based performance metric. *J Neural Eng* 11: 016008, 2014. doi:10.1088/1741-2560/11/1/016008.
41. **Drost G**, **Stegeman DF**, **van Engelen BGM**, **Zwarts MJ.** Clinical applications of high-density surface EMG: a systematic review. *J Electromyogr Kinesiol* 16: 586–602, 2006. doi:10.1016/j.jelekin.2006.09.005.
42. **Aimonetti J-M**, **Vedel J-P**, **Schmied A**, **Pagni S.** Distribution of presynaptic inhibition on type-identified motoneurones in the extensor carpi radialis pool in man. *J Physiol* 522: 125–135, 2000. doi:10.1111/j.1469-7793.2000.t01-1-00125.xm.
43. **Kuznetsova A**, **Brockhoff PB**, **Christensen RHB.** lmerTest package: tests in linear mixed effects models. *J Stat Soft* 82: 1–26, 2017. doi:10.18637/jss.v082.i13.
44. **Wickham H.** *ggplot2: Elegant Graphics for Data Analysis* (2nd ed.). Springer International Publishing, 2016.
45. **Walters SJ**, **Campbell MJ**, **Machin D.** *Medical Statistics: A Textbook for the Health Sciences* (5th ed.). Wiley-Blackwell, 2021.
46. **Rodriguez-Falces J**, **Place N.** Determinants, analysis and interpretation of the muscle compound action potential (M wave) in humans: implications for the study of muscle fatigue. *Eur J Appl Physiol* 118: 501–521, 2018. doi:10.1007/s00421-017-3788-5.
47. **Voigt M**, **Sinkjaer T.** The H-reflex in the passive human soleus muscle is modulated faster than predicted from post-activation depression. *Brain Res* 783: 332–346, 1998. doi:10.1016/S0006-8993(97)01389-9.
48. **Farina D**, **Merletti R.** Estimation of average muscle fiber conduction velocity from two-dimensional surface EMG recordings. *J Neurosci Methods* 134: 199–208, 2004. doi:10.1016/j.jneumeth.2003.12.002.
49. **Guissard N**, **Duchateau J**, **Hainaut K.** Mechanisms of decreased motoneurone excitation during passive muscle stretching. *Exp Brain Res* 137: 163–169, 2001. doi:10.1007/s002210000648.
50. **Clark L**, **O'Leary CB**, **Hong J**, **Lockard M.** The acute effects of stretching on presynaptic inhibition and peak power. *J Sports Med Phys Fitness* 54: 605–610, 2014.
51. **Rudomin P**, **Schmidt RF.** Presynaptic inhibition in the vertebrate spinal cord revisited. *Exp Brain Res* 129: 1–37, 1999. doi:10.1007/s002210050933.
52. **Hari K**, **Lucas-Osma AM**, **Metz K**, **Lin S**, **Pardell N**, **Roszko DA**, **Black S**, **Minarik A**, **Singla R**, **Stephens MJ**, **Pearce RA**, **Fouad K**, **Jones KE**, **Gorassini MA**, **Fenrich KK**, **Li Y**, **Bennett DJ.** GABA facilitates spike propagation through branch points of sensory axons in the spinal cord. *Nat Neurosci* 25: 1288–1299, 2022. doi:10.1038/s41593-022-01162-x.
53. **Metz K**, **Matos IC**, **Hari K**, **Bseis O**, **Afsharipour B**, **Lin S**, **Singla R**, **Fenrich KK**, **Li Y**, **Bennett DJ**, **Gorassini MA.** Post-activation depression from primary afferent depolarization (PAD) produces extensor H-reflex suppression following flexor afferent conditioning. *J Physiol* 601: 1925–1956, 2023. doi:10.1113/JP283706.
54. **Budini F**, **Christova M**, **Gallasch E**, **Rafolt D**, **Tilp M.** Soleus H-reflex inhibition decreases during 30 s static stretching of plantar flexors, showing two recovery steps. *Front Physiol* 9: 935, 2018. doi:10.3389/fphys.2018.00935.
55. **Bringman CL**, **Shields RK**, **DeJong SL.** Corticospinal modulation of vibration-induced H-reflex depression. *Exp Brain Res* 240: 803–812, 2022. doi:10.1007/s00221-022-06306-w.
56. **Stachowski NJ**, **Dougherty KJ.** Spinal inhibitory interneurons: gatekeepers of sensorimotor pathways. *Int J Mol Sci* 22: 2667, 2021. doi:10.3390/ijms22052667.
57. **Behm DG**, **Alizadeh S**, **Drury B**, **Granacher U**, **Moran J.** Non-local acute stretching effects on strength performance in healthy young adults. *Eur J Appl Physiol* 121: 1517–1529, 2021. doi:10.1007/s00421-021-04657-w.
58. **Behm DG**, **Kay AD**, **Trajano GS**, **Blazevich AJ.** Mechanisms underlying performance impairments following prolonged static stretching without a comprehensive warm-up. *Eur J Appl Physiol* 121: 67–94, 2021. doi:10.1007/s00421-020-04538-8.
59. **Heckman CJ**, **Enoka RM.** Motor unit. *Compr Physiol* 2: 2629–2682, 2012. doi:10.1002/cphy.c100087.
60. **Trajano GS**, **Blazevich AJ.** Static stretching reduces motoneuron excitability: the potential role of neuromodulation. *Exerc Sport Sci Rev* 49: 126–132, 2021. doi:10.1249/JES.0000000000000243.
61. **Mesquita RNO**, **Taylor JL**, **Trajano GS**, **Škarabot J**, **Holobar A**, **Gonçalves BAM**, **Blazevich AJ.** Effects of reciprocal inhibition and whole-body relaxation on persistent inward currents estimated by two different methods. *J Physiol* 600: 2765–2787, 2022. doi:10.1113/JP282765.
62. **Trajano GS**, **Taylor JL**, **Orssatto LBR**, **McNulty CR**, **Blazevich AJ.** Passive muscle stretching reduces estimates of persistent inward current strength in soleus motor units. *J Exp Biol* 223: jeb229922, 2020. doi:10.1242/jeb.229922.
63. **Lee RH**, **Heckman CJ.** Adjustable amplification of synaptic input in the dendrites of spinal motoneurons in vivo. *J Neurosci* 20: 6734–6740, 2000. doi:10.1523/JNEUROSCI.20-17-06734.2000.
64. **Miyahara T**, **Hagiya N**, **Ohyama T**, **Nakamura Y.** Modulation of human soleus H reflex in association with voluntary clenching of the teeth. *J Neurophysiol* 76: 2033–2041, 1996. doi:10.1152/jn.1996.76.3.2033.
65. **Takahashi T**, **Ueno T**, **Ohyama T.** Modulation of H reflexes in the forearm during voluntary teeth clenching in humans. *Eur J Appl Physiol* 90: 651–653, 2003. doi:10.1007/s00421-003-0943-y.
66. **Didier H**, **Assandri F**, **Gaffuri F**, **Cavagnetto D**, **Abate A**, **Villanova M**, **Maiorana C.** The role of dental occlusion and neuromuscular behavior in professional ballet dancers' performance: a pilot study. *Healthcare (Basel)* 9: 251, 2021. doi:10.3390/healthcare9030251.
67. **Mesquita RNO**, **Taylor JL**, **Trajano GS**, **Holobar A**, **Gonçalves BAM**, **Blazevich AJ.** Effects of jaw clenching and mental stress on persistent inward currents estimated by two different methods. *Eur J Neurosci* 58: 4011–4033, 2023. doi:10.1111/ejn.16158.
68. **Tuncer M**, **Tucker KJ**, **Türker KS.** Influence of tooth clench on the soleus H-reflex. *Arch Oral Biol* 52: 374–376, 2007. doi:10.1016/j.archoralbio.2006.12.011.